Citation for published version:
Jabban, L, Metcalfe, B, Zhang, D & Iravani, P 2020, Pressure Sensitive Skin for Prosthetic Hands: 2D Contact Location Determination Using Output Connections from a Single Side. in *42nd Annual International Conferences of the IEEE Engineering in Medicine and Biology Society: Enabling Innovative Technologies for Global Healthcare, EMBC 2020.*, 9176163, Proceedings of the Annual International Conference of the IEEE Engineering in Medicine and Biology Society, EMBS, vol. 2020-July, IEEE, pp. 4341-4344, 42nd Annual International Conferences of the IEEE Engineering in Medicine and Biology Society, EMBC 2020, Montreal, Canada, 20/07/20. https://doi.org/10.1109/EMBC44109.2020.9176163

DOI:
10.1109/EMBC44109.2020.9176163

Publication date:
2020

Document Version
Peer reviewed version

Link to publication

University of Bath

Alternative formats
If you require this document in an alternative format, please contact:
openaccess@bath.ac.uk

General rights
Copyright and moral rights for the publications made accessible in the public portal are retained by the authors and/or other copyright owners and it is a condition of accessing publications that users recognise and abide by the legal requirements associated with these rights.

Take down policy
If you believe that this document breaches copyright please contact us providing details, and we will remove access to the work immediately and investigate your claim.

Download date: 05. May. 2023

Pressure Sensitive Skin for Prosthetic Hands: 2D Contact Location Determination Using Output Connections from a Single Side

L. Jabban, B. Metcalfe, D. Zhang and P. Iravani

Abstract— **The human hand is a vital component of our interaction with the environment, containing a large number of sensory receptors. The loss of a hand is, therefore, a serious and debilitating injury. Surveys have shown that 98% of users of upper limb prostheses desire to feel the level of force they apply through their prosthetic hands. Developments in tactile sensors have yielded many functional electronic skins. However, their complexity remains a barrier to their use in commercial prosthetic hands. This paper introduces a new design of a simple, flexible pressure sensor using carbon fibre tows as both the sensor and the electrodes. The design results in a dynamic pressure range of 0.35 to 280 kPa in a 25-by-25 mm prototype.**

I. Introduction

The hand is a vital part of everyday interaction with the environment and, therefore, upper-limb amputations result in a drastic impact on the quality of life. It is estimated that there are 3 million people worldwide with upper limb amputations [1]. This has driven the development of prosthetic hands from simple hooks to the more complex biomimetic hands currently available commercially. The mixed uptake of the available prostheses has led to several surveys targeted at understanding the complex needs of upper limb amputees. The results of those studies show that 98% of the users desire to feel the level of force applied by the prosthesis [2].

Providing such sensory feedback starts with suitable sensors that can be integrated into the prosthetic hand. Unlike the rest of the senses, the sense of touch is not formed of localised sensors. On the contrary, it is composed of a high number of sensors spread over a large area. This introduces a challenge in collecting and processing the data from the different sensors spread across the skin [3].

Direct addressing, where separate connections are assigned for each sensor, is the simplest integration method and requires $2 \times M \times N$ connections for an M by N matrix of sensors. Using a passive matrix of electrodes is common in electronic skin applications and reduces the number of connections required to $M+N$ [4]. Active matrix arrangement uses transistors to address each sensor individually [3]. An alternative to the complex integration methods described is to use computational methods such as artificial neural networks and tomography. Sohn, K. et al. used a deep learning neural network to obtain a spatial resolution of 4 mm from a simple sheet of Polydimethylsiloxane (PDMS) with homogeneously dispersed carbon nanotubes using fewer than $M+N$ connections. However, their design requires connections on all four sides of the sensor [5].

A new design of a flexible pressure sensor is introduced in this paper, where carbon fibre tows are used as both the sensing device and electrodes. The sensor's flexibility allows it to be integrated into a prosthetic hand. The design is driven by the anisotropic resistivity and piezoresistive nature of a carbon fibre tow, which enables the detection of location of the applied pressure using $M+1$ connections on one side of the sensor. The key advantage of this design is the low manufacturing cost and reduced number of output connections. This is particularly useful for the application of prosthetic hands as it enables easier integration of the sensors on the finger. Furthermore, the placement of tactile sensors on a glove, rather than the robotic arm, is preferred to reduce the viscoelastic delay caused by the glove. Given that prostheses users tend to replace the glove every 2 years [6], using simple fabrication techniques allows for cheaper gloves to be made for frequent replacement, while allowing the processing unit to be reused.

II. Methods

A. Sensor Design

Carbon fibre (CF) composites have been used extensively in a range of applications due to their desirable mechanical properties, including low density, high chemical stability and remarkable tensile characteristics [7]. However, CF composites are less frequently exploited for their electrical properties. Some of the recent developments in this area include filters for electromagnetic radiation, sensing, and resin curing for space applications [8].

A key characteristic of unidirectional CF tows and composites is their anisotropic conductivity. The individual fibres provide conduction paths along the longitudinal direction. However, for the current to flow across the width or thickness of the tow, it has to pass through different fibres at their contact points. Several studies have shown the ability to detect damage in CF composites using the longitudinal and transverse resistance measurements [9], [10].

L. Jabban (lj386@bath.ac.uk), B. Metcalfe and D. Zhang are with the Department of Electronic and Electrical Engineering, University of Bath, Bath BA2, UK.

P. Iravani is with the Department of Mechanical Engineering, University of Bath, Bath BA2, UK.

The proposed sensor design, shown in Figure 1, exploits this property by using the longitudinal and through-thickness resistance of the CF to determine the location and magnitude of the applied forces. When pressure is applied, the concentration of the CF strands increases at the contact area, reducing the resistance. The magnitude of the applied pressure can be determined through the change in resistance, and the location of the contact can be determined through a comparison of the different resistance readings across the material as the magnitude of resistance change in R1 and R4 is different to R2-R4 due to the anisotropic resistivity.

The sensor fabrication consists of 5 steps:

1) The piezoresistive mixture is made by mixing 100 µm milled CF (15 wt.%) and PDMS (Sylgard 184).

2) A thin layer of the piezoresistive mixture is applied to the ground tow and left handing for 30 minutes to remove excess material.

3) The ground tow is cured at 60°C for 20 minutes.

4) The sensing tow is placed on top of the piezoresistive layer.

5) The full sensor is cured at 60°C for 40 minutes.

A 25-by-25 mm sensor was produced using the procedure described above. The readings from the sensor were obtained by measuring the voltage between the ground tow and the four outputs (A-D in Figure 1(C)).

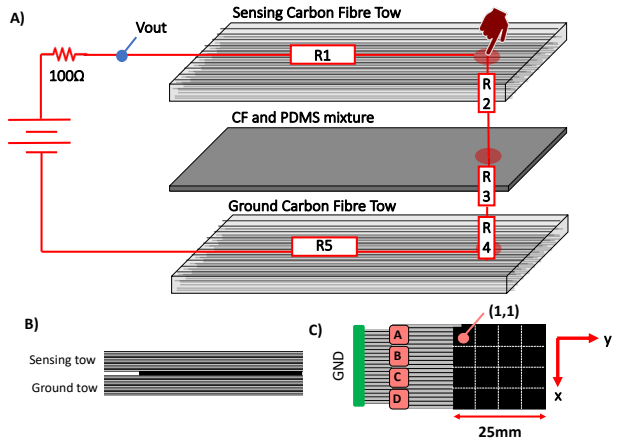

Figure 1. A) Illustration of sensing mechanism. B) side view illustration C) Top view illustration showing the outputs A-D.

B. Sensor Characterisation

In order to characterise the sensor, pressure was applied to the sensor at different locations using a Cartesian robot. The robot enables the location in the *x*-,*y*- and *z*-axis to be controlled, as well as the rate of movement. A strain gauge, connected to an HX711 amplifier, was used to log the applied pressure. The 4 sensor readings were measured via a potential divider. Data acquisition was run in MATLAB in real time.

1) Detection of Pressure location

The sensor is, effectively, made of numerous fibres acting as miniature sensors that cannot be addressed individually. Neural networks (NN) have been used with similar sensor designs to determine the location of the applied force [5]. In order to classify the location of the applied pressure, the surface of the sensor was divided into taxels, forming a 4-by-4 matrix, shown in Figure 1 (C). The *x*- and *y*-location of the applied pressure were determined using two separate NN with a single hidden layer each (Single Layer Perceptron with a sigmoid transfer function), as shown in Figure 2. The rationale behind the choice of two NN is that different relationships are used to determine the location on the *x*- and *y*-axis. Using one NN to classify the location would result in 16 possible outcomes, an increased number of layers required, and, therefore, increased computational cost. The four sensor readings are input to the neural network and the output is the location on either of the axes.

The automated data collection setup, described in *B*, was used to apply a range of pressure levels at different locations on the sensor. The sensor readings and location of applied pressure (*x* and *y*) were stored to be used as training data for the neural network. The number of neurons in the hidden layer was increased until no improvement in the performance was observed.

C. Determining the Applied Force

When pressure is applied at a particular location, the sensor reading corresponding to the appropriate *x*-axis location is expected to show the greatest change in resistance, and therefore, voltage. Furthermore, a change in the *y*-axis location results in a change in R1 and R5 that results in a change in the voltage range that maps onto the pressure range. Due to this, the pressure value is calculated after the contact location is determined, using the voltage reading corresponding to its *x*-axis location. For example, reading A is used for taxel (1,1).

Hysteresis is one of the main problems encountered when using elastic tactile sensors. It is caused by the viscoelastic properties of the polymers used, such as PDMS. Hysteresis results in a difference in the response of the sensor based on whether the applied force is increasing or decreasing and makes it difficult for the applied pressure to be determined directly from a voltage measurement. A hysteresis correction solution proposed by Sanchez-Duran based on the generalised Prandtl-Ishlinskii (PI) model was used to counter this effect [11].

1) Generalised Prandtl-Ishlinskii model

The generalised PI model can be used to describe asymmetrical hysteresis cycles using the generalised play operator (PO) [12]. The output of the model is obtained by integrating the product of the density function $p(r)$ and the generalised play operator $H_r[x](t)$ over a range of threshold r_i between 0 and R, as described by equation (1) [11].

$$y_{PI=} \int_{i=0}^{R} p(r_i)\, H_r[x](t)\, dr \qquad (1)$$

2) Inverse of the generalized Prandtl-Ishlinskii model

The PI model was used to describe the output of the sensor (voltage) for a given applied force. In order to get the force applied from a voltage measurement, the model was inverted. The inverse model was obtained using the inverse of the envelope functions as shown in (2) and (3) [13].

$$x_{PI}= \begin{cases} \gamma_l^{-1} \int_{j=0}^{Q} g(q_j)\, F_q[y](t)dq \text{ for } \dot{y}\geq 0 \\ \gamma_r^{-1} \int_{j=0}^{Q} g(q_j)\, F_q[y](t)dq \text{ for } \dot{y}<0 \end{cases} \quad (2)$$

$$F_q^+[y](t)= max[\, y(t)-q,\ min[y(t)+q\,, F_q(t-1)]] \quad (3)$$

Where q_i is the threshold of the inverse, and $g(q_j)$ is the corresponding density function [13].

3) Selection of model parameters

The selection of PI model parameters, X, which result in the lowest error between the measurement values and model output can be found using an optimisation function (4), where X contains the model parameters and N is the number of data points. The optimisation problem was solved using the *lsqnonlin* function, which is part of MATLAB's Optimisation toolbox.

$$J(X)= \sum_{n=1}^{N} (Y_{PI}(t_n)-y(t_n))^2 \quad (4)$$

Different model parameters are required to describe the relationship between force and voltage for different taxels. Therefore, the optimisation process has to be repeated for each taxel.

III. Results

A. Pressure range

The sensor was able to detect pressures between 0.35 kPa and 280 kPa. The upper limit of the pressure was due to the capabilities of the test rig rather than the sensor. However, this range is considered adequate as the average pressure exerted on the hand when handling tools is below 250 kPa [14].

B. Identification of Contact Location

Plots of force against voltage for different taxels were produced to confirm the hypothesis about how the contact location can be identified. Row 1 and Column 1 (Figure 3 A and B) were chosen to show the change in the outputs as the contact point is moved along the *x*- and *y*-axis, respectively. The processed voltage in A is the voltage divided by the mean voltage of that reading. It can be seen that, as expected, the change in resistance is highest in the output corresponding to the *x*-location of the applied force. As the contact point moves along the *y*-axis, the values of R1 and R5 (refer to Figure 1) increase, and the effect of the change in resistance is reduced as the overall resistance is increased, as can be seen in B. Comparing the resistance of the output corresponding to the *x*-axis location to the rest of the outputs can enable the *y*-axis location to be determined.

Two single-layer neural networks with 150 neurons in the hidden layer were trained to classify the contact location in the *x*- and *y*-direction. A data set of 7800 samples were split into 70% training, 15% validation and 15% testing. MATLAB's pattern recognition function, *nprtool*, was used to train the neural networks to achieve the results shown in Figure 2. Accuracies of 86.3% and 79.6% were achieved for the detection of the *x*-axis and *y*-axis locations, respectively. It can be seen in the confusion matrix that most of the misclassifications were in the neighbouring locations. It can also be seen that the middle classes show lower accuracies. When pressure is applied to the middle of the sensor, for example at (2,2), significant change in resistance is seen in R1-R3. On the other hand, pressure applied at (1,1) will only result in a significant change in R1 and R2, making it easier to distinguish, and therefore classify.

C. Prandtl-Ishlinskii model results

The PI model was used with the readings from taxel (1,1) to produce the graph shown in Figure 3 (C), which shows clear hysteresis. A reduced range of pressures was covered (350 g results in 122.5 kPa applied pressure). This was due to the slipping of the tool used to apply the pressure at high pressures, resulting in a change in the shape of the hysteresis response. The optimisation function was used to find the parameters, X. Those parameters were then used to obtain the value of the applied pressure using the voltage readings. It can be seen that the model matched the measurement values closely. Plotting the result of the hysteresis compensation (Figure 3 (D)) shows a high coefficient of determination, R^2, of 0.98.

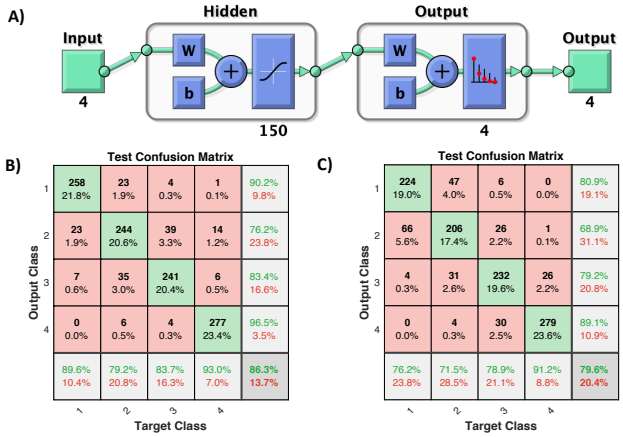

Figure 2. A) Neural network used for the classification of contact location. B) Results for location on x-axis and C) y-axis.

IV. Discussion and Conclusion

The results show that unidirectional carbon fibre can be used to produce flexible, durable and low-cost tactile sensors. Its anisotropic resistivity enables it to act as both the sensor and electrode. However, as with other simple fabrication sensors, post processing is required to produce accurate and precise measurements.

Using neural networks enabled the identification of the contact location of the applied force based on the comparison of the different sensor outputs (A-D). While this method works for contact with objects with small surface areas, it is predicted that correct identification of the *y*-axis location will become more challenging with increased contact area and length of the sensor. Furthermore, using signals from one side might not enable the identification of multiple contact points.

Hysteresis compensation using the inverse PI model resulted in a nearly linear mapping of the calculated force against the measured force. This model was based on a uniform rate of increase and decrease in applied pressure, for a specific contact location. The particular model to be used should be chosen based on the identified contact location.

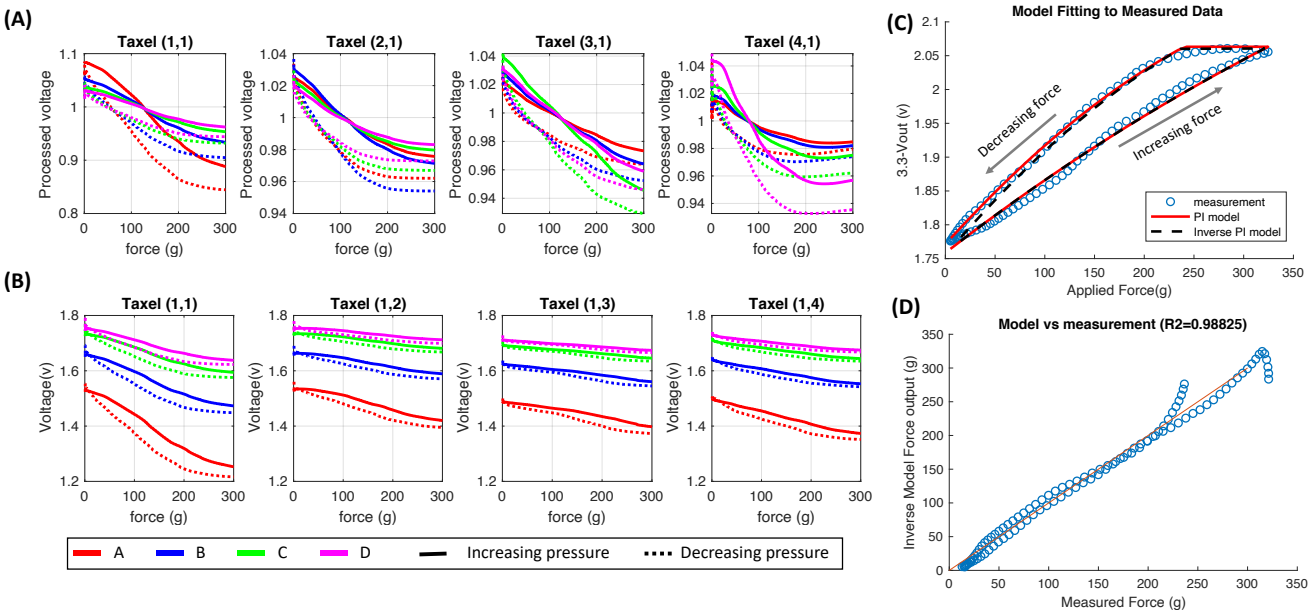

Figure 3. (A,B) The effect of the *x*- and *y*-axis location on the sensor outputs, respectively. Processed voltage is voltage/ mean voltage. (C) Results of the PI model and inverse based on measurements from taxel (1,1) . (D) Hysteresis compensation plot.

Future work will include further investigation into the capabilities and limitations of the sensor. This includes testing the contact location identification using different objects, and the effect of the rate of force application on the shape of the hysteresis curves. Although existing research states that describing rate-dependent asymmetric hysteresis through modelling is not possible, it has been shown that recurrent neural networks, such as long short-term memory recurrent networks (LSTM NN) can be used to obtain relatively accurate force measurements [15]. It is predicted that a solution combining the use of LSTM NN to select the relevant model parameters and the inverse PI model could be suitable for this application.

The ability to use unidirectional CF for tactile sensing opens up a range of design opportunities that could be compared. CF composites are readily available in different configurations, including weaves and 45° biaxial layers, due to their commercial use for their structural capabilities. Another aspect of the future work would be to test the use of 45° biaxial CF to enable 2D measurements with higher resolution.

This paper has shown that a unidirectional CF can serve as both the sensor and electrodes for pressure sensitive skins. Only 5 connections are required on one side of a 25-by-25 mm sensor to determine the location of applied pressure with a resolution of 6 mm and an accuracy of, at least, 79.6%. It also shows that a modified version of the inverse PI model can be used for clockwise hysteresis compensation with R^2 of 0.98.

REFERENCES

[1] P. Taylor, 'Electrical stimulation of the upper limb', 2017.

[2] C. H. Jang *et al.*, 'A survey on activities of daily living and occupations of upper extremity amputees.', *Ann. Rehabil. Med.*, vol. 35, no. 6, pp. 907–21, Dec. 2011.

[3] M. L. Hammock, A. Chortos, B. C. K. Tee, J. B. H. Tok, and Z. Bao, '25th anniversary article: The evolution of electronic skin (E-Skin): A brief history, design considerations, and recent progress', *Adv. Mater.*, vol. 25, no. 42, pp. 5997–6038, 2013.

[4] K. H. Kim, S. K. Hong, N. S. Jang, S. H. Ha, H. W. Lee, and J. M. Kim, 'Wearable Resistive Pressure Sensor Based on Highly Flexible Carbon Composite Conductors with Irregular Surface Morphology', *ACS Appl. Mater. Interfaces*, vol. 9, no. 20, pp. 17499–17507, 2017.

[5] K. S. Sohn *et al.*, 'An extremely simple macroscale electronic skin realized by deep machine learning', *Sci. Rep.*, vol. 7, no. 1, pp. 1–10, 2017.

[6] Y. Yabuki *et al.*, 'Development of new cosmetic gloves for myoelectric prosthetic hand using superelastic rubber', *Rob. Auton. Syst.*, vol. 111, pp. 31–43, 2019.

[7] X. Huang, 'Fabrication and properties of carbon fibers', *Materials (Basel).*, vol. 2, no. 4, pp. 2369–2403, 2009.

[8] N. Athanasopoulos and V. Kostopoulos, 'Prediction and experimental validation of the electrical conductivity of dry carbon fiber unidirectional layers', *Compos. Part B Eng.*, vol. 42, no. 6, pp. 1578–1587, 2011.

[9] Z. H. Xia and W. A. Curtin, 'Modeling of mechanical damage detection in CFRPs via electrical resistance', *Compos. Sci. Technol.*, vol. 67, no. 7–8, pp. 1518–1529, 2007.

[10] M. Ramirez and D. D. L. Chung, 'Electromechanical, self-sensing and viscoelastic behavior of carbon fiber tows', *Carbon N. Y.*, vol. 110, pp. 8–16, 2016.

[11] J. A. Sánchez-Durán, Ó. Oballe-Peinado, J. Castellanos-Ramos, and F. Vidal-Verdú, 'Hysteresis correction of tactile sensor response with a generalized Prandtl-Ishlinskii model', 2011, p. 80662L.

[12] M. Al Janaideh, J. Mao, S. Rakheja, W. Xie, and C. Y. Su, 'Generalized Prandtl-Ishlinskii hysteresis model: Hysteresis modeling and its inverse for compensation in smart actuators', in *Proceedings of the IEEE Conference on Decision and Control*, 2008, pp. 5182–5187.

[13] M. Al Janaideh, S. Rakheja, and C. Y. Su, 'An analytical generalized Prandtl-Ishlinskii model inversion for hysteresis compensation in micropositioning control', *IEEE/ASME Trans. Mechatronics*, vol. 16, no. 4, pp. 734–744, Aug. 2011.

[14] C. Hall, 'External pressure at the hand during object handling and work with tools', vol. 20, pp. 191–206, 1997.

[15] M.-Y. Cho, J. H. Lee, S.-H. Kim, J. S. Kim, and S. Timilsina, 'An Extremely Inexpensive, Simple, and Flexible Carbon Fiber Electrode for Tunable Elastomeric Piezo-Resistive Sensors and Devices Realized by LSTM RNN', *ACS Appl. Mater. Interfaces*, vol. 11, no. 12, pp. 11910–11919, Mar. 2019.